Study of Alloy Disorder in Quantum Dots through Multi-million Atom Simulations

G. Klimeck*, F. Oyafuso*, T. B. Boykin**, R. C. Bowen*, and P. von Allmen*

* Jet Propulsion Laboratory
4800 Oak Grove Dr. MS 169-315, Pasadena, CA, 91109, gekco@jpl.nasa.gov
** University of Alabama at Huntsville, Huntsville, AL, USA

ABSTRACT

A tight binding model which includes s, p, d, and s^* orbitals is used to examine the electronic structures of an ensemble of dome-shaped $In_{0.6}Ga_{0.4}As$ quantum dots. Given ensembles of identically sized quantum dots, variations in composition and configuration yield a linewidth broadening of less than 0.35 meV, much smaller than the total broadening determined from photoluminescence experiments. It is also found that the computed disorder-induced broadening is very sensitive to the applied boundary conditions, so that care must be taken to ensure proper convergence of the numerical results. Examination of local eigenenergies as functions of position shows similar convergence problems and indicates that an inaccurate resolution of the equilibrium atomic positions due to truncation of the simulation domain may be the source of the slow ground state convergence.

Keywords: quantum dot, boundary condition, linewidth, disorder

1 INTRODUCTION

Envelope function-based models such as **k.p** are often used to characterize the electronic structures of quantum dots. Such jellium-like models are often very useful and are not too computationally demanding. However, they suffer as the minimum feature size approaches the length scale of several nanometers or less [1], [2] and also cannot capture effects such as alloy disorder or interface interdiffusion that arise from the discreteness of the underlying medium. The two primary alternative approaches to model solids on finer length scales are tight-binding and pseudopotential methods. We have pursued the former approach for our ability to leverage previous Nanoelectronic Modeling (NEMO) developments [3]–[5], and are currently developing an atomistic nanoelectronic simulation tool (NEMO-3D) to model quantum dot structures on high performance commodity clusters (Beowulfs). Modeling of realistic structures entails simulation domains encompassing many millions of atoms. Such large-scale domains result in very large eigenproblems (dimension $\gtrsim 10^8$) which necessitate the usage of massively parallel computers. Details of the numerical implementation including performance benchmarks have been described in greater detail elsewhere [6].

Our simulation employs a nearest-neighbor tight-binding model ($sp^3d^5s^*$) with a 20 orbital basis, consisting of s, p, and d orbitals, associated with each atomic lattice site. Since the basis set that is used is not complete in a mathematical sense, the parameters that enter the model do not correspond precisely to actual orbital overlaps. Thus, an analytical approach to determine these parameters is insufficient. Instead, a genetic algorithm package is used to determine a set of orbital couplings that reproduces a large number of physical observables of the bulk binary system, including bandgaps and effective masses at various symmetry points in the Brillouin zone. These orbital couplings must also depend on bond lengths to account for the shifts in atomic positions in strained systems. A power-law scaling is assumed (whose exponent is also determined with the genetic algorithm) to account for strain-induced shifts.

Because the basis set used consists of orthogonalized Löwdin orbitals and not the true atomic orbitals, the diagonal (self-coupling) elements are also allowed to vary with the displacement of the nearest neighbor atoms [7]. Since, an accurate calculation of the electronic structure within the tight-binding model also necessitates an accurate representation of the positions of each atom, NEMO-3D uses a valence force field (VFF) model in which the total strain energy, expressed as a local (nearest-neighbor) functional of atomic positions, is minimized [8], [9].

In this work, we examine the dependence of the ground state eigenenergies as a function of various buffer sizes. We shall demonstrate that the variations of eigenenergies can depend strongly on the size of simulation domain, and that proper care must therefore be taken to ensure that a solution has "converged".

2 SIMULATION

2.1 Ground state electron energy

The canonical model used for all the simulations in this work is a dome shape $In_{0.6}Ga_{0.4}As$ quantum dot (QD) of diameter 30 nm and height 5.4 nm embedded in a finite GaAs box. The QD itself contains roughly 2×10^5 atoms. A list of the values of the tight-binding

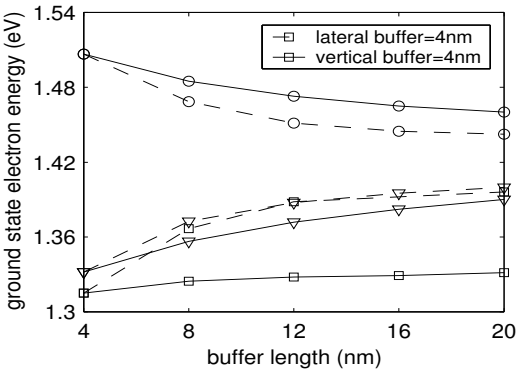

Figure 1: Ground state electron eigenenergies obtained for free, fixed, and periodic boundary conditions. For the case of unconstrained (free) boundary conditions, convergence of eigenenergies is also illustrated for the case of free boundary conditions where only the vertical buffer size is varied and the lateral buffer size is fixed at 4 nm (dashed line).

parameters necessary for the simulation is given in Table III of reference [6]. Although all the QDs are of identical size, the placement of In and Ga cations varies among simulations. We make the ansatz that no correlation in species type exists between any two atomic sites. Thus, sites on the cation sublattice are filled with a 60% (40%) probability of being In (Ga). Note that such an algorithm does not, in general, ensure that exactly 60% of the cations in the QD are In atoms. The resulting broadening of the energy spectrum, then, includes not only the configurational disorder, arising from the distribution of different cations throughout the alloy subject to the constraint of a fixed overall concentration, but also a concentrational disorder that reflects the fact that a growth process never produces nanostructures with identical concentrations each time. It has been demonstrated that for bulk (periodic) systems, the concentrational disorder dominates by an order of magnitude [10]. In the following simulations, we consider three different boundary conditions, fixed, free, and periodic, that directly impact the strain calculation and therefore either indirectly or directly affect the electronic computation. In the fixed case, the surface atoms are constrained to the positions they would have if the simulation domain consisted entirely of GaAs. In the free case, the entire domain is allowed to expand without any external constraints. Finally, under periodic boundary conditions, the total strain energy is minimized with respect to both position and period. In Fig.(1), we compare the ground state electron eigenenergy for each case as a function of buffer size. lso shown is the convergence of eigenenergies for the case of free boundary conditions when only the vertical buffer size is varied and the lateral buffer size is fixed at 4 nm. The largest simulation employs a 16 nm buffer and encompasses approximately six million atoms. Because of memory constraints the buffer sizes in Fig.(1) are limited to 16 nm. The intent is to investigate how well such a truncated system approximates one in which the QD is embedded in an infinitely large block of GaAs. In the case of free boundary conditions no external constraints are imposed, so that the strain computed for the truncated system is reduced from what it should be for an infinite buffer. The shift of the conduction band edge at Γ, which depends linearly on the hydrostatic component, is given by

$$\Delta E_c = \Xi_d^{(000)} \mathrm{Tr}\{\varepsilon\} \quad (1)$$

where $\Xi_d^{(000)} < 0$ [11]. Thus, one expects a reduction in compressive strain (an increase in $\mathrm{Tr}\{\varepsilon\}$) in the QD to accompany a reduction in electron ground state energy. The situation for the fixed case, where the lattice constant on the boundary is constrained to bulk values, is inverted, since the strain effect in the QD is overestimated relative to the case of infinite buffers. Fig.(1) demonstrates that the two cases converge provided that the buffer is made sufficiently large. The periodic case lies in between the other two cases as expected, but yields eigenergies only only slightly greater than for the free case for fixed simulation domain size. Thus, we can expect that the strain computed from the periodic case closely resembles that of the free case. Finally we note that extension of the buffer in the lateral direction for the free case does not significantly alter the computed eigenenergies. This is likely due to the fact that the QD is quite "flat", so that the binding energy is principally determined by confinement in the $\hat{z}$ direction. These results demonstrate that the simulation domain needs to extend rather far into the buffer to assure convergence.

2.2 Linewidth broadening

We now consider the issue of linewidth broadening. That is, given an ensemble of ostensibly identical quantum dots, we explore the fundamental limits of linewidth broadening that arise solely as a result of variations in configurations of cations in the quantum dots and ignore any additional contributions such as size variation, strain-induced spatial perturbations on a QD due to neighboring QDs, and many-body effects. Our calculations for the case of fixed boundary conditions did not yield hole eigenenergies for small buffer sizes, so we consider only the case of free boundary conditions. We examine the electron and hole ground state eigenenergy distributions for three different buffer systems, 4nm 8nm, and 12nm. 190 samples points were obtained for the first two systems and 93 for the larger (and computationally more taxing) 12nm buffer geometry. A histogram of the distributions for the first two geometries is

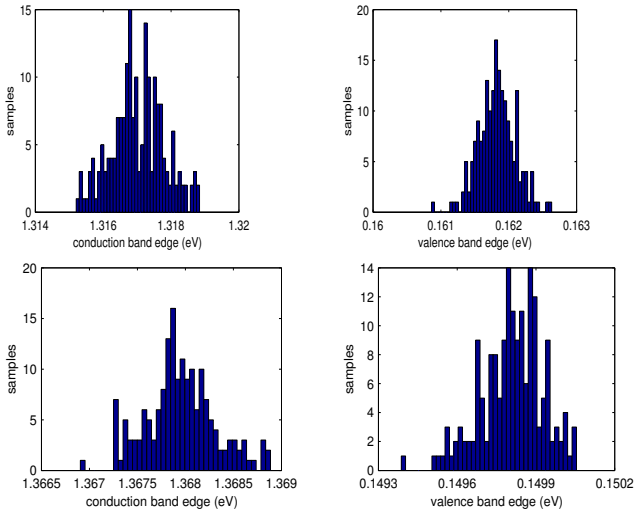

Figure 2: Electron and hole energy distributions for a set of QD with 4 nm (top) and 8 nm (bottom) buffers.

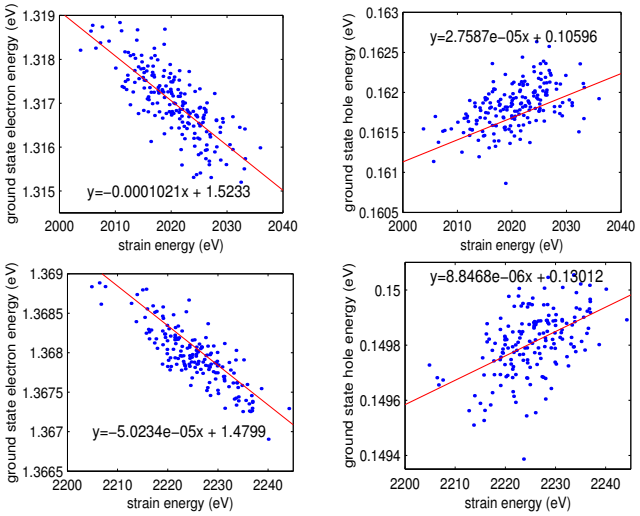

Figure 3: Electron and hole ground state eigenenergies as a function of total strain energy of the QD for a lateral buffer size of 4nm and transverse buffer sizes of 4 nm (top two figures) and 8 nm (bottom two figures) under free boundary conditions.

Table 1: buffer size dependence of eigenenergies and broadening

Statistical data (energies are in meV and lengths are in nm)						
L_{buff}	E_c	σ_c	E_v	σ_v	E_g	σ_{cv}
4	1317.0	0.78	161.8	0.27	1155.2	1.00
8	1368.0	0.36	149.8	0.12	1218.1	0.46
12	1389.4	0.27	141.7	0.14	1247.6	0.35

shown in Fig.(2), and Table (1) summarizes the statistical data for all three configurations. First we note that the electron (hole) energies are shifted up (down) with bigger buffers as found earlier. However, the electron eigenenergy broadening, given by the standard deviation, σ_c, is two to three times larger than that of holes, σ_v. This result differs from an earlier finding for bulk unstrained $Al_xGa_{1-x}As$ with periodic boundary conditions applied in which the electron broadening was found to be only slightly larger than that of holes [10]. This discrepancy might possibly be due the fact that both light and heavy holes are broadened in the bulk unstrained case, while the confinement of a QD splits the Γ_5 degeneracy. Interestingly, the degree to which the electron and hole distributions are broadened is strongly dependent on the buffer size. Indeed, it seems likely that a significant broadening of the eigenenergy distribution is an artifact of the truncation of the simulation domain, since increasing the simulation size reduces the broadening. One possible explanation for this reduction in linewidth is that as eigenstates are pushed up closer to the bulk GaAs conduction and valence band edges, perturbations to concentration and strain produce less significant changes to the eigenvalues.

Finally, note that the sum of electron and hole standard deviations is still (roughly) equal to the standard deviation of the energy gap. This result indicates that the electron and hole eigenenergies are strongly correlated. This is not unexpected since the concentrational broadening had previously been identified to be the most dominant effect in bulk unstrained systems [10]. Another way to see this correlation is to look at the dependence of the eigenenergies on the total strain energy of the system, which also depends on the alloy concentration. In the VFF model used, the total strain energy is the sum over all atoms of the local strain energy at each atom, which depends only on the positions of the neighboring atoms. Fig.(3) shows scatter plots for electron and hole ground state energies as a function of total strain for two different lateral buffer widths of 4 and 8 nm. The strain energies (not shown) seem to have a roughly Gaussian shape with a spread of approximately 25 eV (or about 1 %). Notice that an increase in strain energy reduces the band gap. The reduction in band gap is reasonable, since an increase in strain energy is likely a result of a slightly higher concentration of In atoms. The trends are the same for both buffer sizes, except that the strain energy for the system with the 4 nm buffer is reduced, since the overall system size is smaller. However, the *slopes* of the curves are much larger for the smaller buffer, indicating a stronger dependence of eigenergy on strain.

2.3 Local bandstructure

We next examine the effect of the deformation of the primitive cells under strain on the local electron and hole band structure within the GaAs buffer. At each cation (Ga) site, we define a "local" eigenenergy obtained by

computing the band minima at Γ of a bulk solid constructed from the single primitive cell formed by the cation and its four neighboring As anions. In essence, these local eigenenergies define a spatially dependent band edge. It is important to note that the eigenenergy local to a cation depends only on the relative position of the surrounding As atoms. Thus, these local eigenvalues essentially reflect local strain conditions. Fig.(4) shows local eigenvalues of the buffer material for our canonical problem with the three boundary conditions discussed earlier and with buffer sizes of 4nm, 8nm, and 12nm. Here, larger dot size corresponds to larger buffer size. In each case, local eigenvalues are computed about each

cation contained within a narrow tube aligned along a lateral (x) direction that passes close to axes of maximal symmetry. The tube extends from the edge of the enclosing buffer up to the QD, and it was verified that the behavior of the eigenvalues in buffer at the other end was symmetric, due to the reflection symmetry of the system. The finite thickness of the tube accounts for the spreading of the local eigenvalues as one moves from the edge of the simulation domain toward the quantum dot. Note that for none of the boundary conditions is a buffer of 4 nm is sufficient to characterize the QD, since the local eigenergies at the boundary of the simulation domain are not close to the bulk eigenvalue of 1.424 eV. However, convergence toward this bulk value is evident as the buffer size is increased. For both periodic and free boundary conditions, the eigenvalues are pushed down from their bulk values, whereas for the fixed boundary condition case, the eigenvalues obtained are greater than that of bulk GaAs. Since the shift in the CB edge (at Γ) arises only from the hydrostatic component of the strain, as indicated by Eq.(1), tensile strain should lower E_c. This was confirmed in figure 7 of [6] which also shows that E_c is reduced under biaxial tension. For very small buffers under free boundary condition, GaAs unit cells on the surface should stretch out biaxially to match the larger $In_{0.6}Ga_{0.4}As$ lattice constant. This tension should also be present under periodic boundary condition, and, is in fact reflected in the reduced value of E_c for both of those cases. For the case of fixed boundary condition, the boundary is constrained to positions that it would have if the entire simulation domain were composed of GaAs. In this case, the presence of InGaAs in the interior should compress the GaAs buffer on the outside. This compressive strain increases the value of E_c as seen in Fig.(4).

The convergence of hole eigenenergies, shown in Fig.(5), demonstrates behavior similar to that seen for electrons, except that light hole and heavy hole splitting of roughly 10 meV is evident even for the largest buffer size. The loss of degeneracy arises from the symmetry breaking due to strain. For the smallest buffer of 4 nm, the splitting is found to be as large as 90 meV for the case of periodic boundary conditions. Furthermore, even for the largest buffer size, the local eigenergies "flatten out" and saturate to an asymptotic value that differs from unstrained GaAs. This suggests that the inaccurate characterization of the strain may be the principal limitation on the accuracy of the "global" eigenvalues.

3 conclusion

The convergence of electron and hole ground states of a dome-shaped $In_{0.6}Ga_{0.4}As$ quantum dot has been explored within an $sp^3d^5s^*$ tight binding model. It has been demonstrated that within this model, one must include a barrier region many times the size of the embedded quantum dot. The inadequate convergence of the local bandstructure is a direct reflection of the lack of convergence of the strain, and may be the principal cause for the slow convergence of the "global" ground state eigenenergies.

4 acknowledgement

The work described in this publication was carried out at the Jet Propulsion Laboratory, California Institute of Technology. The Beowulf cluster on which our calculations were performed was provided by funding from the NASA Offices of Earth Science, Aeronautics, and Space Science.

REFERENCES

[1] T.G. Dargam, R.B. Capaz, and B. Koiller, *Phys. Rev. B* **56** p. 9625, (1997)

[2] H. Fu, Lin-Wang, and A. Zunger, *Phys. Rev. B* **57**, p. 9971, (1998).

[3] R.C. Bowen, W.R. Frensley, G. Klimeck, and R. Lake, *Phys. Rev. B*, **52**, p.2754 (1995)

[4] G. Klimeck, R. Lake, R.C. Bowen, W. Frensley, and T. Moise, *Appl. Phys. Lett.*, **67**, p.2539 (1995)

[5] R.C. Bowen, G. Klimeck, R. Lake, W.R. Frensley, and T. Moise, *J. Appl. Phys*, **81**, p3207 (1997)

[6] G. Klimeck, F. Oyafuso, T. Boykin, R. C. Bowen, and P. von Allmen, *Computer Modeling in Engineering & Sciences*, **3**, p. 601, (2002)

[7] T. Boykin et al., *submitted to Phys. Rev. B*

[8] P. Keating, *Phys. Rev.*, **145**, 637 (1966)

[9] C. Pryor et al, *J. of Appl. Phys.*, **83**, 2548 (1998)

[10] F. Oyafuso et al, *to appear in J. Computational Electronics*

[11] P. Bhattacharya, *Indium Gallium Arsenide*, vol. 8, INSPEC, London, 1993

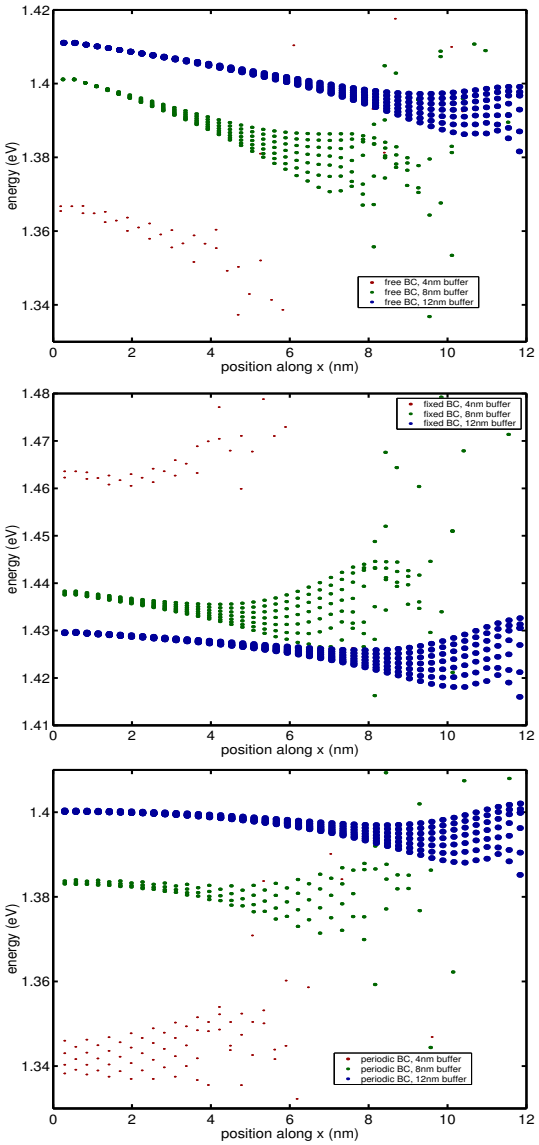

Figure 4: Local electron eigenenergies of the GaAs buffer along a lateral axis of the QD for different boundary conditions and buffer sizes of 4nm, 8nm, and 12 nm. Larger dot size corresponds to larger buffer size.

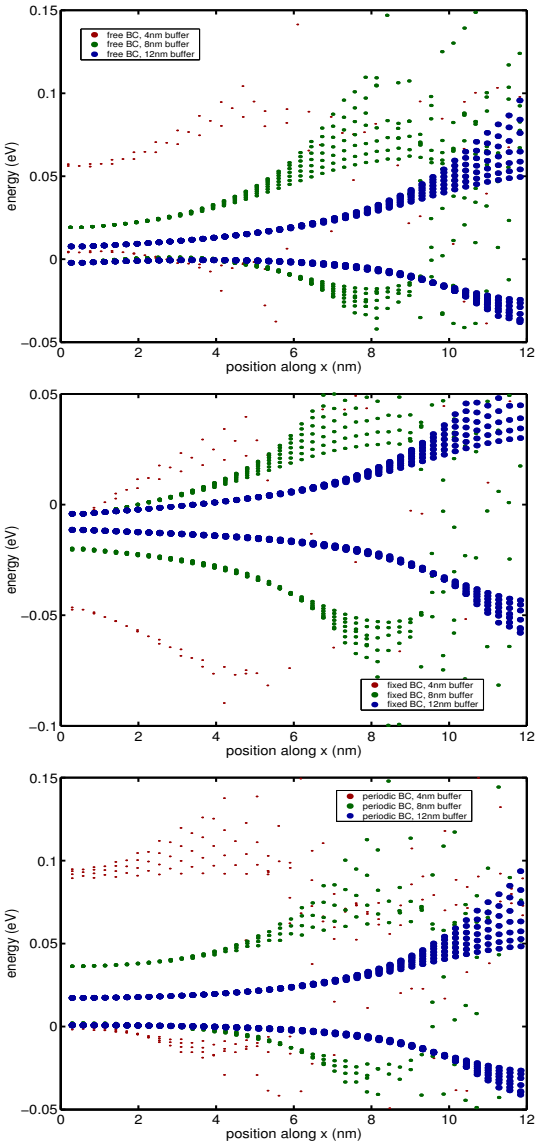

Figure 5: Local hole eigenenergies of the GaAs buffer along a lateral axis of the QD for different boundary conditions and buffer sizes of 4nm, 8nm, and 12 nm. Larger dot size corresponds to larger buffer size.